Proceedings of the
47th IEEE Conference on Decision and Control
Cancun, Mexico, Dec. 9-11, 2008

Modeling and Analysis of Auto-Tapping AFM

Michele Basso, Paolo Paoletti, Bruno Tiribilli and Massimo Vassalli

Abstract— **The paper presents a new Atomic Force Microscopy setup where the cantilever gets excited by a positive feedback loop containing a saturation function. The proposed scheme can be easily modeled and analyzed in the frequency domain using harmonic balance techniques. In imaging applications, we show that an additional controller for the saturation threshold can further reduce the topography error. Preliminary results in experiments confirm the effectiveness of this operating mode, providing good topography resolution and removing some of the known drawbacks of standard dynamic setups.**

I. INTRODUCTION

Since its invention in 1986 [1], atomic force microscopy (AFM) has been widely used as a tool for investigating material characteristics at a nanoscale level. In particular, it has been used for topographic measurements, in order to obtain surface images of the sample. A typical AFM setup is depicted in Fig. 1: a sharp tip on top of a flexible cantilever interacts with the sample and the topography can be recovered by measuring the cantilever deflection via a four-quadrants opto-detector. A piezoelectric actuator is eventually in charge of moving vertically the sample in order to maintain a constant force between the tip and the sample.

In tapping mode, another piezoelectric actuator, called "dither piezo", is mounted at the cantilever base and induces harmonic oscillations of the cantilever via acoustic excitation [2]. Since the amplitude of the above oscillations decreases as the tip gets closer to the sample, a feedback controller regulates the sample distance in order to maintain a set-point oscillation amplitude during the scanning. Tapping mode AFM presents several advantages with respect to either contact and non-contact operating modes [3], one of the most important being the ability to obtain measures with a significantly decreased mean interaction force and lateral shear [4]. One of the major drawbacks of tapping mode AFM is the need to identify in advance the cantilever resonance frequency. In fact the cantilever has to be externally excited at a frequency that must be close to the resonance one. The identification of the cantilever resonance frequency is a time-consuming task and can be quite difficult in liquid environments due to the presence of "multiple peaks" in the cantilever frequency response [5]. Moreover, the scanning rate is primarily limited by the performance of the piezoelectric actuator and by the high Q factor of typical cantilever when operating in air [6].

M. Basso and P. Paoletti are with Dipartimento di Sistemi e Informatica, Università di Firenze, via S.Marta 3, I-50139, Firenze (Italy) basso@dsi.unifi.it, paolo.paoletti@dsi.unifi.it

B. Tiribilli and M.Vassalli are with Istituto dei Sistemi Complessi, CNR, via Madonna del Piano 10, I-50019, Sesto Fiorentino, Firenze (Italy) bruno.tiribilli@isc.cnr.it, massimo.vassalli@isc.cnr.it

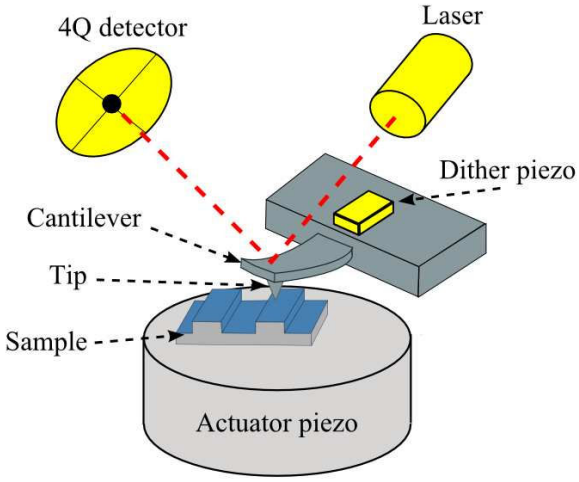

Fig. 1. Simplified AFM setup.

In this work we present a new working mode – hereafter denoted as auto-tapping – that preserves the benefits of tapping mode and greatly reduces the above mentioned drawbacks. More specifically, the dither piezo is now driven by a positive feedback of the cantilever deflection signal which induces self-sustained oscillations. The amplitude of such oscillations can be regulated by a specific saturation function. Although the idea of using a positive feedback of the cantilever deflection is not new [5], [7], it has not been exploited yet to design a practical and simple setup to be employed in imaging applications, similarly to those used in standard tapping mode AFMs. Moreover, a specific model of auto-tapping is proposed which can be effectively analyzed in the frequency domain by using harmonic balance techniques.

The paper is organized as follows. In Section II a suitable model of the AFM in the new operating mode is presented and analyzed via harmonic balance techniques, in Section III we propose an additional control scheme exploiting the saturation threshold that increases the dynamical response of auto-tapping. Finally, in Section IV we illustrate some preliminary experimental results which confirm the validity of the proposed technique.

II. MODEL

A typical description of the AFM cantilever dynamics is based on the approximation provided by a second-order

978-1-4244-3124-3/08/$25.00 ©2008 IEEE

harmonic oscillator [8] whose frequency response is given by the expression

$$L(j\omega) = \frac{Y(j\omega)}{F(j\omega)} = \frac{1}{\omega_n^2 - \omega^2 + 2j\zeta\omega_n\omega}, \qquad (1)$$

where $Y(j\omega)$ and $F(j\omega)$ are, respectively, the Fourier transforms of the cantilever deflection $y(t)$ and of the force $f(t)$ (per unit mass) applied to the tip, ω_n indicates the natural frequency, and ζ is the cantilever damping factor. The natural frequency ω_n is related to the cantilever spring constant K_c and to the cantilever mass m by the relation

$$\omega_n^2 = \frac{K_c}{m}, \qquad (2)$$

whereas the value of the damping ζ depends essentially by the environment where the instrument operates. In fact, ζ can be negligible in vacuum or air, while it is very significant when the AFM works in liquids.

As already mentioned in the introduction, it has been experimentally observed that self-sustained oscillations of the cantilever can be induced by feeding the dither piezo with a signal proportional to the cantilever deflection. Particular care must be taken in order to model the loop that is responsible of the birth of such oscillations in auto-tapping mode AFM. Classical linear feedback theory excludes that a positive feedback of the system dynamics in (1) is able to generate stable oscillations, since the cantilever equilibrium remains stable even for large gains. Various experiments considering the frequency response of the cantilever excited through the dither piezo show the presence of a phase shift between system input and output. This phenomenon can be physically explained by the transmission delay of the acoustic excitation of the tip. In this scenario, an increase of the feedback gain can lead to an unstable equilibrium for the cantilever dynamics when a pair of complex poles crosses the imaginary axis. The corresponding equilibrium will then result in an unstable focus such that all trajectories spiral out of the origin. The presence of the dither piezo saturation naturally limits the system trajectories which then converge to a stable oscillation (a limit cycle) whose amplitude directly depends on the saturation level. Therefore, the above saturation nonlinearity is well suited to explain the occurrence of a self-sustained oscillation and can be interpreted by taking into account that the dither piezo provides a limit in the force that can exert on the cantilever base.

According to these hypotheses, the excitation force on the tip can be expressed as

$$f(t) = \Psi \text{sat}\left[\Omega y(t-\tau)\right]. \qquad (3)$$

In (3) we indicate with the symbol Ω the measurement converting factor (i.e. the conversion gain between the deflection in nm and the voltage fed to the dither piezo), with Ψ the actuator factor (i.e. the gain value related to the mechanical coupling between the dither piezo and the cantilever base), with τ the delay time and with $\text{sat}(\cdot)$ the saturation function.

If the sample is also taken into account, we define as "separation" the distance l between the sample surface and the center of the cantilever oscillation. Moreover, we assume that the cantilever-sample interaction can be expressed by means of a force F_h that depends essentially upon the tip-sample distance, that is, the cantilever deflection plus the separation. Accordingly, the behavior of the system is thus governed by the following differential equation

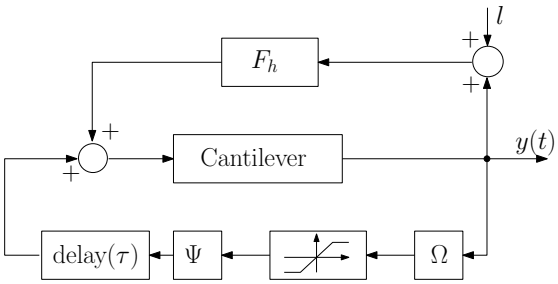

Fig. 2. Block diagram of auto-tapping mode.

$$\ddot{y}(t) + 2\zeta\omega_n\dot{y}(t) + \omega_n^2 y(t) = \Psi \text{sat}\left[\Omega y(t-\tau)\right] + F_h(y+l) \qquad (4)$$

which is also reported as a schematic in Fig. 2. Note that this is a typical example of a Lur'e system [9], i.e. a feedback interconnection of a linear dynamical system and a nonlinear block represented, respectively, by the cantilever and by the loops containing the saturation and the tip-sample interaction force.

A. Model analysis via harmonic balance

When the atomic force microscope operates in (auto) tapping mode, one can experimentally observe that the cantilever oscillation is quasi-sinusoidal since the strongly peaked second order dynamics of the cantilever filters out most of the higher harmonics. Therefore, we can approximate the deflection by

$$y(t) = B\cos(\omega t) \qquad (5)$$

and use a first order harmonic balance technique to study the system oscillations [9]. More specifically, we can refer to the schematic of Fig. 3 and associate to every nonlinear block $n(\cdot)$ the so-called "describing function" defined as

$$N(B,\omega) = \frac{B_1 + jA_1}{B} \qquad (6)$$

where B_1 and A_1 are the first order terms of the Fourier series of the output of the nonlinear block $n(\cdot)$ fed with $B\cos(\omega t)$, i.e.

$$\begin{aligned} B_1 &= \frac{2}{T}\int_0^T n\left[B\cos(\omega t)\right]\cos(\omega t)dt \\ A_1 &= \frac{2}{T}\int_0^T n\left[B\cos(\omega t)\right]\sin(\omega t)dt\ . \end{aligned} \qquad (7)$$

The describing function associated to the saturation block

$$n(y) = \begin{cases} -s & y \le -s \\ y & |y| < s \\ s & y \ge s \end{cases} \qquad (8)$$

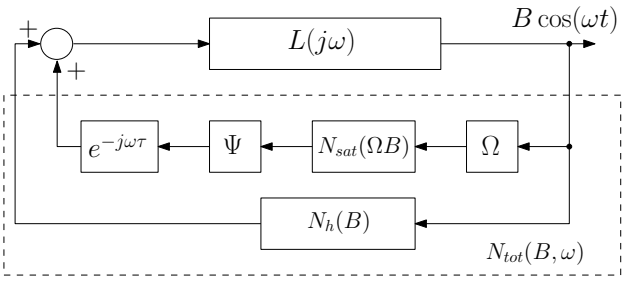

Fig. 3. Harmonic balance analysis for auto-tapping mode.

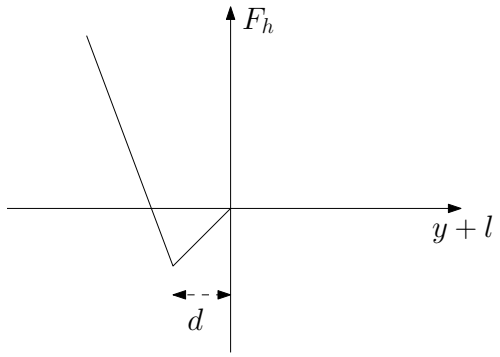

Fig. 4. Piecewise linear approximation of the tip-sample interaction.

where s represents the saturation threshold, has the expression (see, for example [9])

$$N_{sat}(B) = \begin{cases} 1 & B \le s \\ \frac{2}{\pi}\left(\sin^{-1}\left(\frac{s}{B}\right) + \frac{s}{B}\sqrt{1-\frac{s^2}{B^2}}\right) & B > s \end{cases} . \tag{9}$$

There exist several different representations which model the interaction between the tip and the sample, typical examples are Lennard-Jones potentials [10] and Hertz contact models [11]. Although the following analysis could be conducted with these models, for the sake of simplicity we choose the following piecewise linear approximation of these forces as depicted in Fig. 4

$$F_h = \begin{cases} 0 & y+l > 0 \\ s_a^2(y+l) & -d < y+l \le 0 \\ s_a^2(y+l) - s_r^2(y+l+d) & y+l \le -d \end{cases} . \tag{10}$$

This approximation is able to capture the most important characteristic of the tip-sample interaction: far away from the sample the interaction force is negligible, when the tip approaches the sample there is a small region where there exists an attractive force (linear with slope s_a^2 in the model), if the separation further decreases a repulsive force due to atomic repulsion is exchanged between the tip and the sample (slope $s_a^2 - s_r^2$ in the model). The describing function of the

TABLE I
NUMERICAL SIMULATION PARAMETER VALUES

Name	Value	Unit
ω_n	414690	rad/s
ζ	0.0017367	
τ	101	μs
B_0	65	nm
s_0	1	V
Ω_0	0.0196	V/nm
Ψ	0.0346	$nm/\mu s^2$
d	3	nm
s_a	0.15	μs^{-1}
s_r	3.6	μs^{-1}
B_r	55	nm
K_{sat}^-	0.0073	V/nm
K_{sat}^+	0.11	V/nm

nonlinearity in 10 can be expressed as [9]

$$N_h(B) = \frac{1}{\pi}\left[s_a^2 Re\left\{ \cos^{-1}\left(\frac{l}{B}\right) - \frac{l}{B}\sqrt{1-\left(\frac{l}{B}\right)^2} \right\} + \right.$$
$$\left. - s_r^2 Re\left\{ \cos^{-1}\left(\frac{l+d}{B}\right) - \frac{l+d}{B}\sqrt{1-\left(\frac{l+d}{B}\right)^2} \right\} \right] \tag{11}$$

. Finally, we can compute the overall describing function $N_{tot}(B,\omega)$ as a combination of the blocks of Fig. 3 which yields

$$N_{tot}(B,\omega) = N_h(B) + \Psi N_{sat}(\Omega B)\Omega e^{-j\omega\tau} . \tag{12}$$

Conditions for the existence of autonomous oscillations $B\cos(\omega t)$ are obtained by imposing that the feedback gain along the loop is unitary, which yields the so-called harmonic balance equation

$$L(j\omega)N_{tot}(B,\omega) = 1 \tag{13}$$

to be solved in the unknowns B and ω, as a function of the system parameters. The analytical solution of this equation can be a very difficult task, therefore we choose to solve it numerically. The parameter values used for the harmonic balance analysis and the subsequent simulations are reported in Table I. First of all, we note that, far away from the sample where $F_h = 0$, we can easily decompose the real and imaginary parts of (13). By solving the imaginary part equation we can exploit a direct relationship between the free oscillation frequency and the delay time τ, that is

$$\omega = \frac{1}{\tau}\angle L(j\omega). \tag{14}$$

Moreover, by solving the real part equation, we conclude that the cantilever oscillation amplitude far away from the sample depends essentially on the saturation threshold s and it is not much influenced by the gain value Ω, as one could expect at a first glance. In Fig. 5 and Fig. 6 we report the dependence of the oscillation amplitude on the values of Ω (normalized with

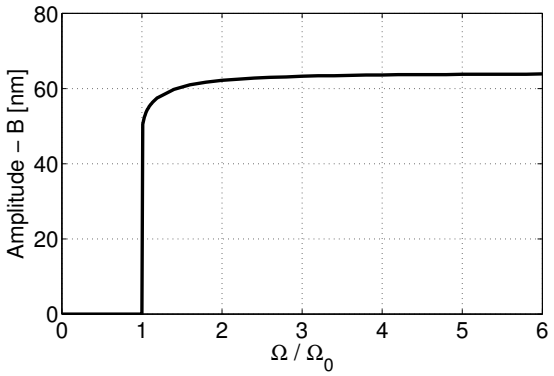

Fig. 5. Free oscillation amplitude vs. gain value Ω.

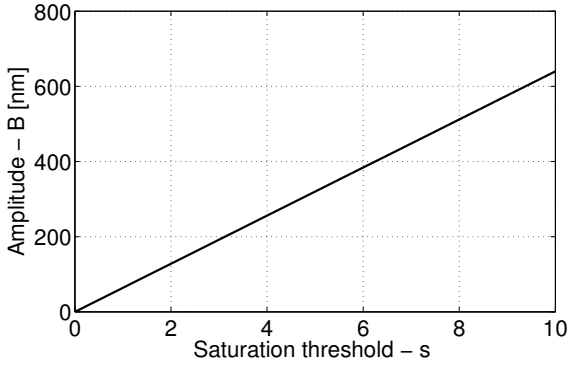

Fig. 6. Free oscillation amplitude vs. Saturation threshold.

respect to the critical gain Ω_0 which provides the onset of the self-sustained oscillations) and the threshold s, respectively. Note that the relationship between the saturation threshold and the free oscillation amplitude is quasi-exactly linear, so that s can be used to easily tune this amplitude. The gain value Ω can be used to switch on or off the oscillation and can be tuned by modulating the laser intensity or external amplifier gain during experiments.

When the tip approaches the sample surface the value of F_h is no longer zero, inducing amplitude and frequency changes on the cantilever oscillation. In particular, the attracting region in Fig. 4 generates a small increase in the oscillation amplitude, whereas the repulsion region generates an amplitude decrease (see Fig. 7). It is important to note that, in this latter region, there exists a linear dependence of the amplitude with respect to the separation, similarly to what happens in classical tapping mode [12]. This linear relationship is very useful since it allows to employ the same piezo control system designed for tapping mode.

In Fig. 8 we report some results obtained by numerical integration of Eq. (4) subject to the force (10). The simulations are performed at different scan rates on a reference sample (a calibration grid) with a step height of $100nm$ and pitch $3\mu m$. It is evident that classical tapping mode and auto-tapping mode have quite similar performance in topography reconstruction, whereas there is a strong degradation at

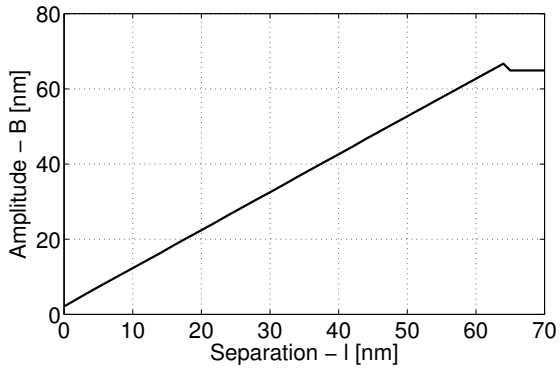

Fig. 7. Cantilever oscillation amplitude vs. separation.

higher scan velocities. In particular, the falling edge of the sample is not correctly measured since the tip does not interact with the surface for a long time interval, as we will better explain in the next section.

III. SATURATION THRESHOLD CONTROL

The ability to modulate the free oscillation amplitude by means of the saturation threshold can be exploited to increase the performance of the traditional feedback loop that controls the actuator piezo. By doing so, it is possible to achieve better performance in topography and better control of the forces that the cantilever tip applies to the sample. The basic idea is to control the saturation threshold in order to adapt it to the amplitude imposed by the presence of the sample, such that the cantilever oscillation is decreased accordingly to the tip-sample interaction force. Of course, this is the same objective of the piezo scanner controller, although the latter is achieved with a response limited by the piezo bandwidth. Conversely, the saturation threshold regulates the cantilever oscillation amplitude quasi-instantaneously and allows for a better tracking of the sample when fast scan rates are used. A standard piezo controller (usually a PI) is then required only for compensating low-frequency/high-amplitude topographic changes, such as sample tilts. The resulting control scheme is illustrated in Fig. 9. The saturation controller can be implemented as the simple negative-feedback proportional controller

$$s(t) = s_0 - \frac{s_0}{B_r}[B_r - B(t)], \tag{15}$$

where s_0 represents the nominal threshold value and B_r is the reference amplitude, i.e the set-point of the actuator piezo controller. We can choose s_0 such that the oscillation amplitude far away from the sample (the free cantilever oscillation) is set to a value B_0 not much larger than B_r, in order to reduce tip-sample interaction forces. Moreover, we note that the system behavior is non symmetric between the sample approach and retract phases, since during the former the PI controller operates mainly in open-loop until the tip impacts again the sample surface. This lack of symmetry is particularly evident when the saturation threshold controller is disabled because the oscillation amplitude can

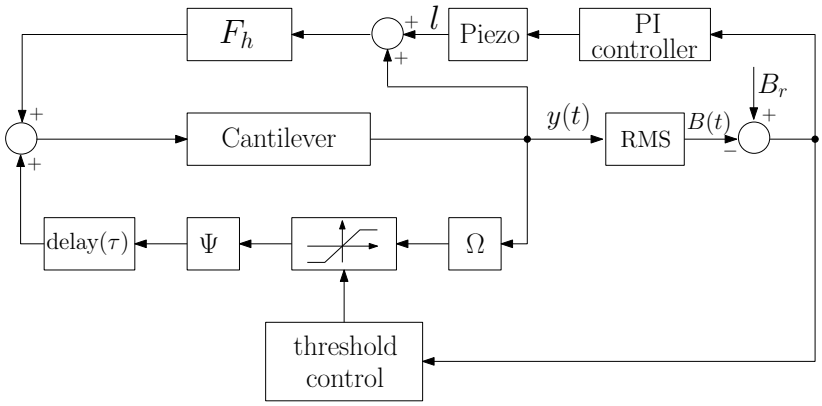

Fig. 9. Saturation threshold control scheme.

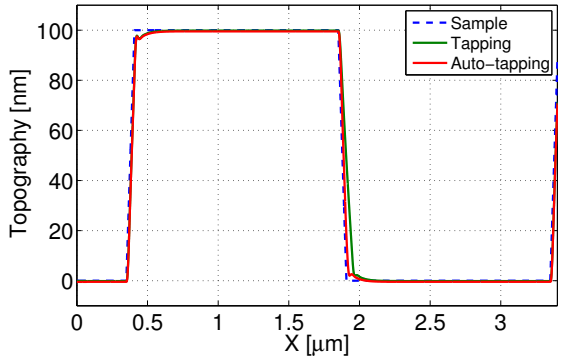

(a)

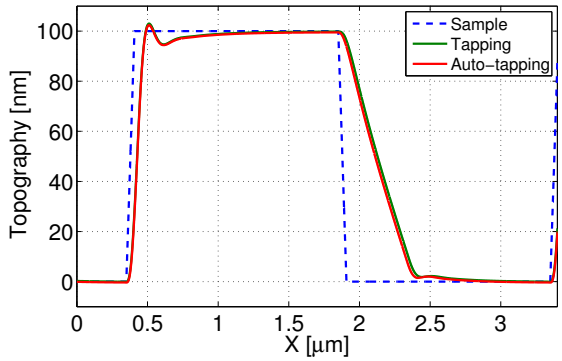

(b)

Fig. 8. Comparison of tapping and auto-tapping scan line profiles with a scan velocity of (a) $3\mu m/s$ and (b) $15\mu m/s$.

not be increased beyond B_0. The same situation is present in classical tapping mode where the maximum amplitude value is determined by the dither piezo excitation strength, see for example [13]. This effect can be only reduced by setting B_r far smaller than B_0 which, in turn, leads to higher mean tip-sample interaction forces. The saturation threshold controller overcomes this problem since it forces the cantilever to oscillate at higher amplitudes thanks to the ability to increase the free oscillation amplitude above B_0.

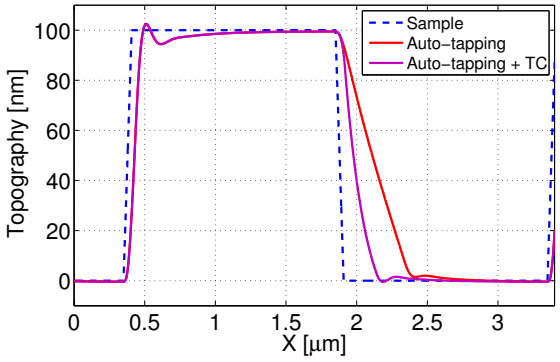

Fig. 10. Comparison of auto-tapping single line profiles with and without saturation threshold control (scan velocity of $15\mu m/s$).

Therefore, the time interval when the PI controller operates in open-loop is greatly reduced and depends essentially upon the dynamics of the saturation controller and the settling time of the cantilever oscillation which are much faster than the actuator piezo dynamics. In order to further reduce the interval with the piezo controller operating in open-loop, it can be useful to introduce two different gains, one for the sample approach phase and the other for the sample retract phase, i.e.

$$s(t) = \begin{cases} s_0 - K^-_{sat}(B_r - B(t)) & B_r - B(t) > 0 \\ s_0 - K^+_{sat}(B_r - B(t)) & B_r - B(t) < 0 \end{cases} \tag{16}$$

with $K^-_{sat} \leq s_0/B_r \leq K^+_{sat}$, such that the oscillation amplitude is strongly increased during the approach phase. In Fig. 10 we report a comparison between the simulation results for the auto-tapping model with and without saturation threshold control (the model parameters are taken from Table I, threshold controller from (16)), showing a faster response during the approach phase.

IV. EXPERIMENTAL RESULTS

The proposed control setup has been tested in a AFM prototype system where the cantilever support has been equipped with a small piezo ($5mm \times 5mm \times 0.65mm$)

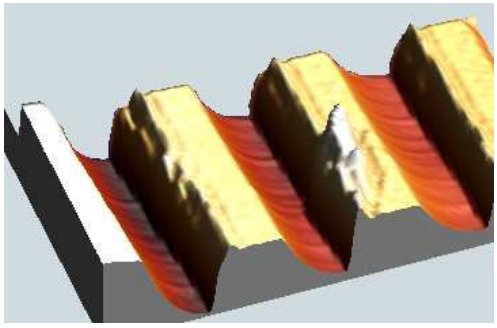

(a)

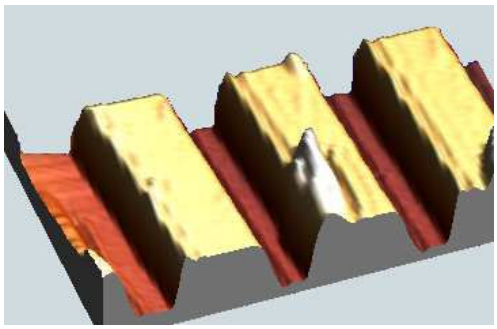

(b)

Fig. 11. Comparison of experimental images: (a) auto-tapping, (b) auto-tapping with threshold control.

providing acoustic excitation. We used a "non-contact" type AFM probe (model NCLR by NANOSENSORS Neuchatel, Switzerland) with $\omega_n = 1.011 \cdot 10^6 rad/s$ and $K_c = 31 \div 71 N/m$. In order to make a direct comparison between classical tapping mode and the proposed auto-tapping mode, we employed the commercial controller SPMagic R2 (by Elbatech srl) as scanning piezo controller. The control law indicated in (16) was implemented via a real-time Linux PC system based on the RTAI-XML platform [14]. The reference sample was a standard calibration grating TGZ02 (by MikroMash, Tallin, Estonia) with known pitch $3\mu m$, and step height $100nm$. The images were obtained by the WSxM software [15].

In Fig. 11 we report a comparison between images obtained in auto-tapping mode with and without the saturation controller enabled. The free oscillation amplitude B_0 was set at about $60nm$, while the actuator piezo controller reference was set at about $40nm$, the scanning velocity was $10\mu m/s$, with a scanning area of $5 \times 10\mu m$ and grid resolution of 128×256 pixel. Note that the presence of the saturation threshold controller allows for much better performance in topography reconstruction.

V. CONCLUSIONS

In this paper we have presented an analysis of a new modality for topographic measurements via atomic force microscopy, called "auto-tapping". Starting from experimental evidence, we have proposed a model that correctly describes the system behavior and allows for a detailed analysis via harmonic balance techniques. Exploiting some peculiar features of the analyzed model, we have proposed an enhanced control scheme that guarantees better performance in topography reconstruction. Preliminary results of experiments have shown that the proposed setup can be effectively employed in imaging applications with a number of advantages with respect to classical techniques.

REFERENCES

[1] G. Binnig, C. F. Quate, and C. Gerber, "Atomic force microscope," *Phys. Rev. Lett.*, vol. 56, no. 9, pp. 930–933, Mar 1986.

[2] C. A. J. Putman, K. O. V. der Werf, B. G. D. Grooth, N. F. V. Hulst, and J. Greve, "Tapping mode atomic force microscopy in liquid," *Applied Physics Letters*, vol. 64, no. 18, pp. 2454–2456, 1994.

[3] S. Das, P. Sreeram, A. K. Raychaudhuri, T. P. Sai, and L. K. Brar, "Non-contact dynamic mode atomic force microscope: Effects of nonlinear atomic forces," in *2006 IEEE Conference on Emerging Technologies - Nanoelectronics*, 2006.

[4] J. Tamayo, A. D. L. Humphris, and M. J. Miles, "Piconewton regime dynamic force microscopy in liquid," *Applied Physics Letters*, vol. 77, no. 4, pp. 582–584, 2000.

[5] A. D. L. Humphris, J. Tamayo, and M. J. Miles, "Active quality factor control in liquids for force spectroscopy," *Langmuir*, vol. 16, pp. 7891–7894, 2000.

[6] T. Kowalewski and J. Legleiter, "Imaging stability and average tip-sample force in tapping mode atomic foce microscopy," *Journal of Applied Physics*, vol. 99, p. 064903, 2006.

[7] A. Passian, G. Muralidharan, S. Kouchekian, A. Mehta, S. Cherian, T. L. Ferrell, and T. Thundat, "Dynamics of self-driven microcantilevers," *Journal of Applied Physics*, vol. 91, pp. 4693–4700, 2002.

[8] T. R. Rodriguez and R. Garcia, "Tip motion in amplitude modulation (tapping-mode) atomic-force microscopy: Comparison between continuous and point-mass models," *Applied Physics Letters*, vol. 80, no. 9, pp. 1646–1648, 2002.

[9] H. K. Khalil, *Nonlinear System*. Prentice Hall, 2002.

[10] M. Lee and W. Jhe, "General theory of amplitude-modulation atomic force microscopy," *Physical Review Letters*, vol. 97, no. 3, p. 036104, 2006.

[11] J. Domke and M. Radmacher, "Measuring the elastic properties of thin polymer films with the atomic force microscope," *Langmuir*, vol. 14, no. 12, pp. 3320–3325, 1998.

[12] M. V. Salapaka, D. J. Chen, and J. P. Cleveland, "Linearity of amplitude and phase in tapping-mode atomic force microscopy," *Phys. Rev. B*, vol. 61, pp. 1106–1115, 2000.

[13] T. Sulchek, R. Hsieh, J. D. Adams, G. G. Yaralioglu, S. C. Minne, C. F. Quate, J. P. Cleveland, A. Atalar, and D. M. Adderton, "High-speed tapping mode imaging with active Q control for atomic force microscopy," *Applied Physics Letters*, vol. 76, no. 11, pp. 1473–1475, 2000.

[14] M. Basso, R. Bucher, M. Romagnoli, and M. Vassalli, "Real-time control with linux: A web services approach," *Decision and Control, 2005 and 2005 European Control Conference. CDC-ECC '05. 44th IEEE Conference on*, pp. 2733–2738, 12-15 Dec. 2005.

[15] I. Horcas, R. Fernández, J. M. Gómez-Rodríguez, J. Colchero, J. Gómez-Herrero, and A. M. Baro, "Wsxm: A software for scanning probe microscopy and a tool for nanotechnology," *Review of Scientific Instruments*, vol. 78, no. 1, p. 013705, 2007.